Supplement of Atmos. Chem. Phys., 19, 3493–3513, 2019
https://doi.org/10.5194/acp-19-3493-2019-supplement

Atmospheric Chemistry and Physics
Open Access

Supplement of

Daytime atmospheric oxidation capacity in four Chinese megacities duringthe photochemically polluted season: a case study based on box model simulation

Zhaofeng Tan et al.

Correspondence to: Keding Lu (k.lu@pku.edu.cn) and Yuanhang Zhang (yhzhang@pku.edu.cn)

Modelled nitrate production using ISORROPIA model.

The gas-particle partitioning is calculated by the aerosol thermodynamic model (ISORROPIA). The ISORROPIA-II thermodynamic equilibrium model (Clegg et al., 1998) was used to calculate the partition weight of the gas phase and particulate phase (Eq. 4). The input of ISORROPIA-II model includes the total soluble ions concentrations in gas phase and $PM_{2.5}$ (ammonium, nitrate, sulfate and chloride), relative humidity (RH) and temperature (T). The model runs in the backward mode which assumes the aerosol solutions are metastable.

The chemical model and aerosol dynamic model are combined to simulate the time-dependent total nitrate concentration and it's partitioning. The derivative of HNO_3 and pNO_3^- can be expressed as E S1 and E S2, respectively.

$$\frac{\partial HNO_3}{\partial t} = P(HNO_3) - L(HNO_3) + E(NO_3) + \frac{\partial HNO_3}{\partial X}\mu \qquad \text{(E S1)}$$

$$\frac{\partial pNO_3^-}{\partial t} = P(pNO_3^-) - L(pNO_3^-) - E(NO_3) + \frac{\partial pNO_3^-}{\partial X}\mu \qquad \text{(E S2)}$$

The first terms in E S1 and E S2 represent the chemical production rate that can be calculated by the chemical box model. In this study, $P(pNO_3^-)$ is zero because we only consider daytime photochemical production. The second terms denote the loss rate which is mainly dry deposition. The deposition velocity for HNO_3 ($v_d(HNO_3)$) and pNO_3 ($v_d(HNO_3)$) are 7 cm s^{-1} and 2 cm s^{-1} as recommend by (Prabhakar et al., 2017), respectively. The BLH is about 2000 m to represent typical summer boundary layer.

The third terms are the gas-particle equilibrium conversion rate. Although it does not change the total nitrate concentration, it determines the partitioning between HNO_3 and pNO_3^- and thus has change the loss rate because nitric acid and particulate nitrate have different dry deposition rate. When emission and transports are negligible (see below), the equations can be combined and simplified as E S3.

$$\frac{\partial TNO_3}{\partial t} = P(HNO_3) + P(NO_3^-) - L(HNO_3) - L(pNO_3^-) \qquad \text{(E S3)}$$

The partition is assumed to reach equilibrium because the time scale of reaching equilibrium is in range of minutes, 1-2 orders smaller than those of deposition and chemical production (Morino et al., 2006;Neuman et al., 2003). Therefore, the photochemical produced HNO_3 will deposit on to the aerosol if the ambient NH_3 is sufficient. The nitric acid could also lose via deposition. The decomposition rate is set to be 7 cm s^{-1}, which results in a deposition timescale being 8 hours by assuming the boundary layer height to be 2 km (typical values for summertime). The total ammonia (NH_4TOT) is calculated from an iterative method for each case to reproduce the gas-phase NH_3 concentrations reported by Pan et al. (2018). From the field measurements, the averaged NH_3 concentrations were Beijing: 16.3 μg/m^3, Shanghai: 14.6 μg/m^3 (the number is adapted from a close-by city Nanjing), Guangzhou: 5.9 μg/m^3, and Chongqing: 10.5 μg/m^3 (the number is adapted from a close-by city Chengdu) (Pan et al., 2018).

In the base scenario, the other chemical compositions are set to zero (total SO_4^{2-}, Na^+, and Cl^-). The simplification uncertainty is evaluated by the following sensitivity tests. As shown in Table 2, the NH_4NO_3 concentration and the particulate nitrate to total nitrate ratio $\varepsilon(NO_3^-)$ is calculated for different model scenarios. First, if NH_3 concentrations are changed by a factor of 2, the change to partitioning is relatively small in Beijing because the NH_3 concentrations are high. It's worth noting that NH_4NO_3 concentration is still high even if the NH_3 concentration is reduced by two-fold in Beijing, which highlights the difficulty in particulate nitrate reduction. In contrast, the change almost linearly correlates with the change of NH_3 in Guangzhou during the daytime due to the limited amount of NH_3. The role of other anions and cations is investigated by setting the SO_4^{2-} and Na^+ to be 10 μg/m^3, respectively. Since SO_4^{2-} reacts with NH_4^+ and thus competes with the formation of NH_4NO_3. The NH_4NO_3 formation will be limited if NH_3 is not sufficient given the NH_3 to tend to react with SO_4^{2-} before NO_3^-. The nitrate concentrations decrease by 1-3 μg/m^3 when SO_4^{2-} is fixed in all cities to be 10 μg/m^3 during day and night (Table S5). In contrast, additional cations can neutralize more nitrates and enhance the gas-to-particle partitioning. For example, if 10 μg/m^3 of Na^+ is added, stronger nitrate production is found (Table S5). It is caused by two kinds of effect. First, the stronger partitioning enhances the particulate nitrate directly. Second, the total nitrate loss is reduced by less $HNO_{3(g)}$ deposition because more nitrate remains in the particle phase.

Table S1 measured species for ozone pollution analysis and instrument time resolution, accuracy and limit of detection

Species	Method	Time resolution	Accuracy (1σ)	Limit of Detection / ppbv
Photolysis frequencies	Actinic flux spectroradiometry	20 s	±10 %	Five orders of magnitude lower than maximum at noon
O_3	UV absorption	1 min	5%	0.5
NO	Chemiluminescence	1 min	±20 %	60 pptv
NO_2	Chemiluminescence	1 min	±20 %	0.3
CO	IR absorption	1 min	5%	4
VOCs	Gas chromatography and mass spectroscopy /flame ionization detector	1 h	10%~20%	0.01~0.2

Table S2 Summary of measured VOCs concentration for four campaigns

	Beijing			Shanghai			Guangzhou			Chongqing		
VOC / ppbv	**Mean**	**Median**	**Max**	**Mean**	**Median**	**Max**	**Mean**	**Median**	**Max**	**Mean**	**Median**	**Max**
1,2,3-TRIMETHYLBENZENE	0.026	0.022	0.100	0.130	0.120	0.340	0.090	0.065	0.473	0.068	0.053	0.189
1,2,4-TRIMETHYLBENZENE	0.098	0.085	0.370	0.160	0.150	0.610	0.199	0.121	1.140	0.225	0.161	0.756
1,3,5-TRIMETHYLBENZENE	0.022	0.018	0.111	0.004	0.000	0.230	0.077	0.053	0.347	0.079	0.058	0.337
1-BUTENE	0.167	0.140	0.803	0.072	0.060	0.300	0.239	0.218	0.607	0.193	0.146	0.939
1-HEXENE	Nan	Nan	Nan	0.323	0.280	1.870	0.074	0.048	0.429	0.065	0.062	0.193
1-PENTENE	0.025	0.019	0.156	0.049	0.020	0.330	0.049	0.033	0.295	0.057	0.042	0.471
2,2,4-TRIMETHYLPENTANE	0.051	0.045	0.240	0.155	0.130	0.990	0.072	0.039	0.736	0.056	0.045	0.177
2,2-DIMETHYLBUTANE	0.020	0.019	0.070	0.149	0.140	0.410	0.099	0.063	0.898	0.054	0.037	1.236
2,3,4-TRIMETHYLPENTANE	0.021	0.019	0.094	0.023	0.000	0.350	0.045	0.028	0.336	0.026	0.022	0.071
2,3-DIMETHYLBUTANE	0.033	0.028	0.137	0.071	0.070	0.180	0.137	0.072	1.584	0.077	0.058	0.769
2,3-DIMETHYLPENTANE	0.049	0.038	0.469	0.027	0.000	0.490	0.111	0.061	0.667	0.056	0.040	0.353
2,4-DIMETHYLPENTANE	0.039	0.037	0.099	0.112	0.100	0.350	0.070	0.046	0.379	0.030	0.024	0.142
2-METHYLHEPTANE	0.016	0.014	0.050	0.002	0.000	0.210	0.066	0.046	0.440	0.039	0.032	0.162
2-METHYLHEXANE	0.061	0.055	0.227	0.000	0.000	0.000	0.273	0.174	1.391	0.133	0.095	0.976
2-METHYLPENTANE	0.226	0.206	0.983	0.265	0.230	1.610	1.066	0.557	8.730	0.360	0.268	3.827
3-METHYLHEPTANE	0.021	0.019	0.066	0.095	0.100	0.210	0.054	0.037	0.345	0.024	0.020	0.113
3-METHYLHEXANE	0.107	0.093	0.307	0.116	0.110	0.260	0.299	0.177	1.936	0.150	0.101	1.196
3-METHYLPENTANE	0.277	0.252	1.027	0.130	0.110	0.580	0.716	0.378	4.242	0.363	0.259	4.246
BENZENE	0.909	0.780	7.830	0.413	0.350	1.240	0.989	0.560	11.448	1.080	0.995	3.749
CIS-2-PENTENE	0.005	0.004	0.045	0.015	0.000	0.670	0.014	0.007	0.107	0.023	0.005	0.287
CIS-BUTENE	0.035	0.019	0.301	0.003	0.000	0.280	0.122	0.124	0.259	0.143	0.100	1.333
CYCLOHEXANE	0.079	0.058	1.048	0.097	0.080	0.320	0.222	0.103	2.180	0.079	0.064	0.293
CYCLOPENTANE	0.125	0.117	0.355	0.048	0.050	0.150	0.117	0.108	0.313	0.167	0.135	0.716
ETHANE	4.896	4.570	13.941	2.432	2.300	7.570	1.952	1.661	5.029	5.145	4.957	11.305
ETHENE	2.210	2.087	7.887	0.921	0.700	5.290	1.522	1.242	6.875	4.039	3.435	11.949
ETHYLBENZENE	0.335	0.257	1.636	0.355	0.290	1.460	1.322	0.782	16.959	0.625	0.480	2.176
ETHYNE	Nan	Nan	Nan	0.025	0.020	0.130	1.355	1.263	2.949	4.123	3.649	11.352

ISO-BUTANE	1.836	1.747	6.574	0.779	0.650	3.760	1.884	1.536	6.630	0.652	0.542	3.581
ISO-PENTANE	1.414	1.326	3.941	0.691	0.560	3.110	1.205	1.079	5.581	1.987	1.412	34.131
ISO-PROPYLBENZENE	0.011	0.010	0.056	0.033	0.000	0.940	0.047	0.037	0.230	0.032	0.026	0.096
ISOPRENE	0.272	0.208	1.289	0.000	0.000	0.110	0.126	0.088	0.809	0.404	0.332	1.641
M-DIETHYLBENZENE	Nan	Nan	Nan	0.217	0.190	0.820	0.036	0.035	0.181	0.026	0.020	0.088
M-ETHYLTOLUENE	0.052	0.045	0.206	0.033	0.000	0.500	0.168	0.122	0.779	0.150	0.111	0.666
M,P-XYLENE	0.604	0.413	3.006	0.565	0.420	3.180	1.508	0.770	24.621	0.655	0.511	2.352
METHYLCYCLOHEXANE	0.074	0.056	0.344	0.003	0.000	0.460	0.187	0.085	2.100	0.189	0.064	4.341
METHYLCYCLOPENTANE	0.121	0.107	0.399	0.064	0.050	0.190	0.296	0.161	2.022	0.120	0.088	0.776
N-BUTANE	2.579	2.403	8.366	0.770	0.600	3.360	2.790	2.339	9.093	1.050	0.847	6.242
N-DECANE	0.021	0.018	0.093	0.074	0.070	0.270	0.108	0.071	0.544	0.086	0.068	0.206
N-HEPTANE	0.116	0.095	0.386	0.037	0.000	0.310	0.197	0.113	1.420	0.209	0.158	1.230
N-HEXANE	0.232	0.170	1.271	0.414	0.260	2.960	0.975	0.480	7.397	0.469	0.318	3.201
N-NONANE	0.033	0.026	0.187	0.057	0.050	0.270	0.079	0.048	0.434	0.469	0.361	1.607
N-OCTANE	0.046	0.037	0.191	0.100	0.080	0.440	0.107	0.072	0.720	0.091	0.078	0.244
N-PENTANE	0.877	0.762	2.383	0.508	0.480	1.280	0.751	0.626	3.083	0.936	0.657	7.593
N-PROPYLBENZENE	0.023	0.021	0.074	0.065	0.060	0.210	0.067	0.057	0.210	0.059	0.051	0.201
N-UNDECANE	0.033	0.030	0.136	0.011	0.000	0.190	0.094	0.073	0.396	0.133	0.115	0.291
O-ETHYLTOLUENE	0.024	0.021	0.086	0.058	0.050	0.200	0.078	0.057	0.322	0.067	0.055	0.263
O-XYLENE	0.175	0.126	0.933	0.256	0.200	1.270	1.058	0.633	8.043	0.327	0.256	1.176
P-DIETHYLBENZENE	Nan	Nan	Nan	0.000	0.000	0.000	0.071	0.050	0.563	0.054	0.042	0.151
P-ETHYLTOLUENE	0.030	0.025	0.127	0.043	0.040	0.160	0.107	0.076	0.478	0.086	0.070	0.329
PROPANE	3.651	3.456	11.666	2.355	2.130	9.360	4.801	3.754	20.957	1.221	1.121	2.860
PROPENE	0.581	0.496	2.472	0.897	0.870	3.430	0.568	0.358	3.387	0.785	0.717	2.336
STYRENE	0.040	0.026	0.383	0.202	0.170	1.270	0.180	0.079	2.078	0.119	0.084	0.493
TOLUENE	1.319	1.055	6.400	0.867	0.550	5.290	5.312	3.041	39.897	1.154	0.963	3.594
TRANS-2-BUTENE	0.110	0.092	0.470	0.003	0.000	0.260	0.201	0.186	0.395	0.175	0.125	1.851
TRANS-2-PENTENE	0.008	0.003	0.136	0.024	0.000	0.860	0.026	0.011	0.355	0.052	0.008	0.771

Table S3 Summary of measured and modelled species

Species	Parameters
Measured	T, P, RH, photolysis rate, NO, NO_2, O_3, C2-C8 alkanes, C2-C6 alkenes, C6-C10 aromatics
Modelled	OH, HO_2, RO_2, k_{OH}, OVOCs (including formaldehyde, acetaldehyde, methacrolein, other aldydes, glyoxal , acetones, methyl vinyl ketone, other ketones, methanol, ethanol, phenol, formic acid, acetic acid and higher acids, and so on)
Scaled	HONO (=0.02×NO_2)

Table S4 Summary of model senstivity test results

Concentrations	**Base**	**HONO=0.03*NO_2**	**HONO=0.015*NO_2**	**Unscaled HONO**
HONO [ppbv]	0.39, 0.30, 0.52, 0.30	0.57, 0.46, 0.79, 0.46	0.28, 0.23, 0.39, 0.23	0.07, 0.20, 0.10, 0.11
OH [10^6cm^{-3}]	4.0, 3.2, 1.1, 2.6	4.6, 3.5, 1.3, 2.9	3.7, 3.0, 1.1, 2.4	3.0, 3.0, 0.8, 2.1
HO_2[10^8cm^{-3}]	1.2, 0.8, 0.9, 2.3	1.5, 0.9, 1.0, 2.5	1.2, 0.7, 0.9, 2.2	1.0, 0.7, 0.8, 2.0
RO_2[10^8cm^{-3}]	0.9, 0.6, 0.9, 1.7	1.0, 0.6, 1.0, 1.8	0.8, 0.5, 0.9, 1.6	0.8, 0.5, 0.8, 1.4
HCHO [ppbv]	5.2, 4.4, 3.9, 5.5	5.8, 4.6, 4.2, 6.1	4.9, 4.2, 3.7, 5.2	4.1, 4.1, 3.3, 4.6

Table S5 Equilibrium Model sensitivity summary for NH_4NO_3 mass concentration and particulate nitrate to total nitrate ratio $\varepsilon(NO_3^-)$ during daytime (06:00—18:00) and nighttime (00:00—06:00, 18:00—24:00).

	Base		NH_3×2		NH_3 / 2		SO_4^{2-}=10 μg/m^3		Na^+=10 μg/m^3	
	NO_3^- [μg/m^3]	$\varepsilon(NO_3^-)$ [%]	NO_3^- [μg/m^3]	$\varepsilon(NO_3^-)$ [%]	NO_3^- [μg/m^3]	$\varepsilon(NO_3^-)$ [%]	NO_3^- [μg/m^3]	$\varepsilon(NO_3^-)$ [%]	NO_3^- [μg/m^3]	$\varepsilon(NO_3^-)$ [%]
					Beijing					
Day	59	83	77	92	29	58	56	81	60	83
Night	69	96	86	100	41	83	67	96	73	99
					Shanghai					
Day	21	59	39	83	3	16	17	53	31	73
Night	33	92	49	99	15	69	32	91	44	98
					Guangzhou					
Day	13	56	28	83	1	11	11	50	28	82
Night	21	86	34	97	5	39	19	84	32	95
					Chongqing					
Day	16	57	34	83	1	7	14	53	28	76
Night	24	85	40	97	5	36	23	85	35	93

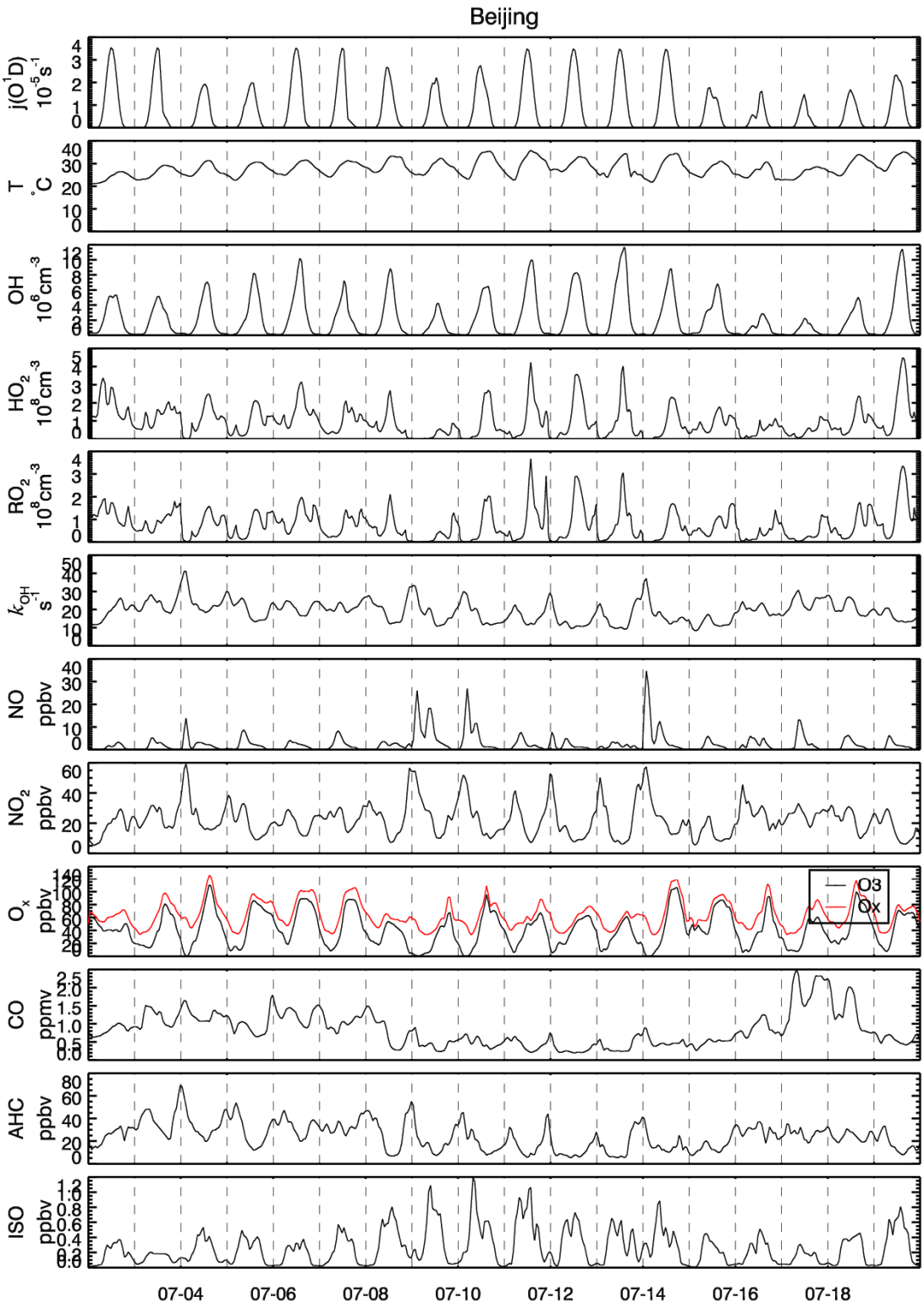

Figure S1 The time series of measured parameters (j(O^1D), Temperature, NO, NO_2, O_3, O_x, CO, AHC, isoprene) and modelled OH, HO_2, and RO_2 concentrations and OH reactivity in Beijing.

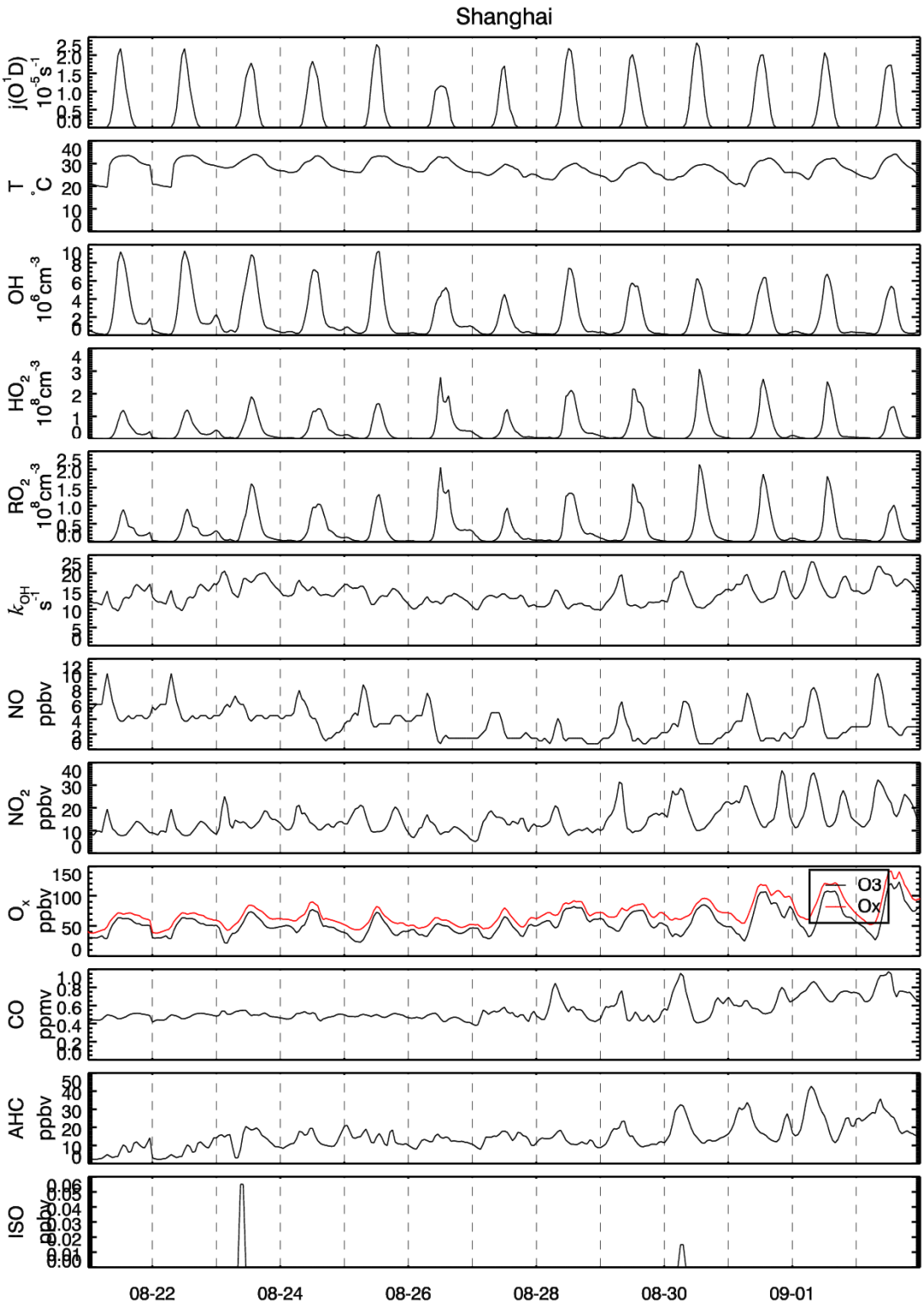

Figure S2 The time series of measured parameters (j(O^1D), Temperature, NO, NO_2, O_3, O_x, CO, AHC, isoprene) and modelled OH, HO_2, and RO_2 concentrations and OH reactivity in Shanghai.

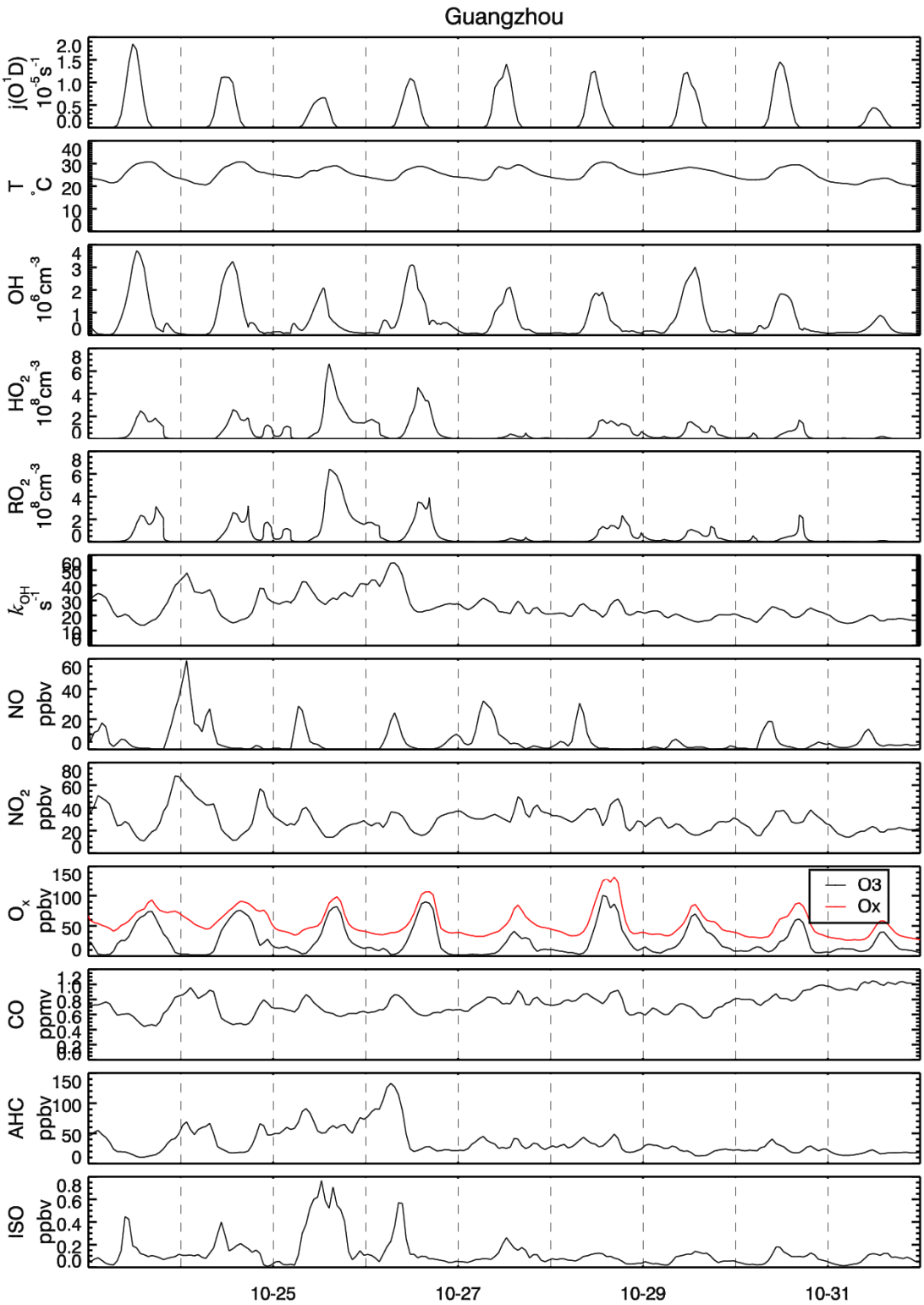

Figure S3 The time series of measured parameters (j(O^1D), Temperature, NO, NO_2, O_3, O_x, CO, AHC, isoprene) and modelled OH, HO_2, and RO_2 concentrations and OH reactivity in Guangzhou.

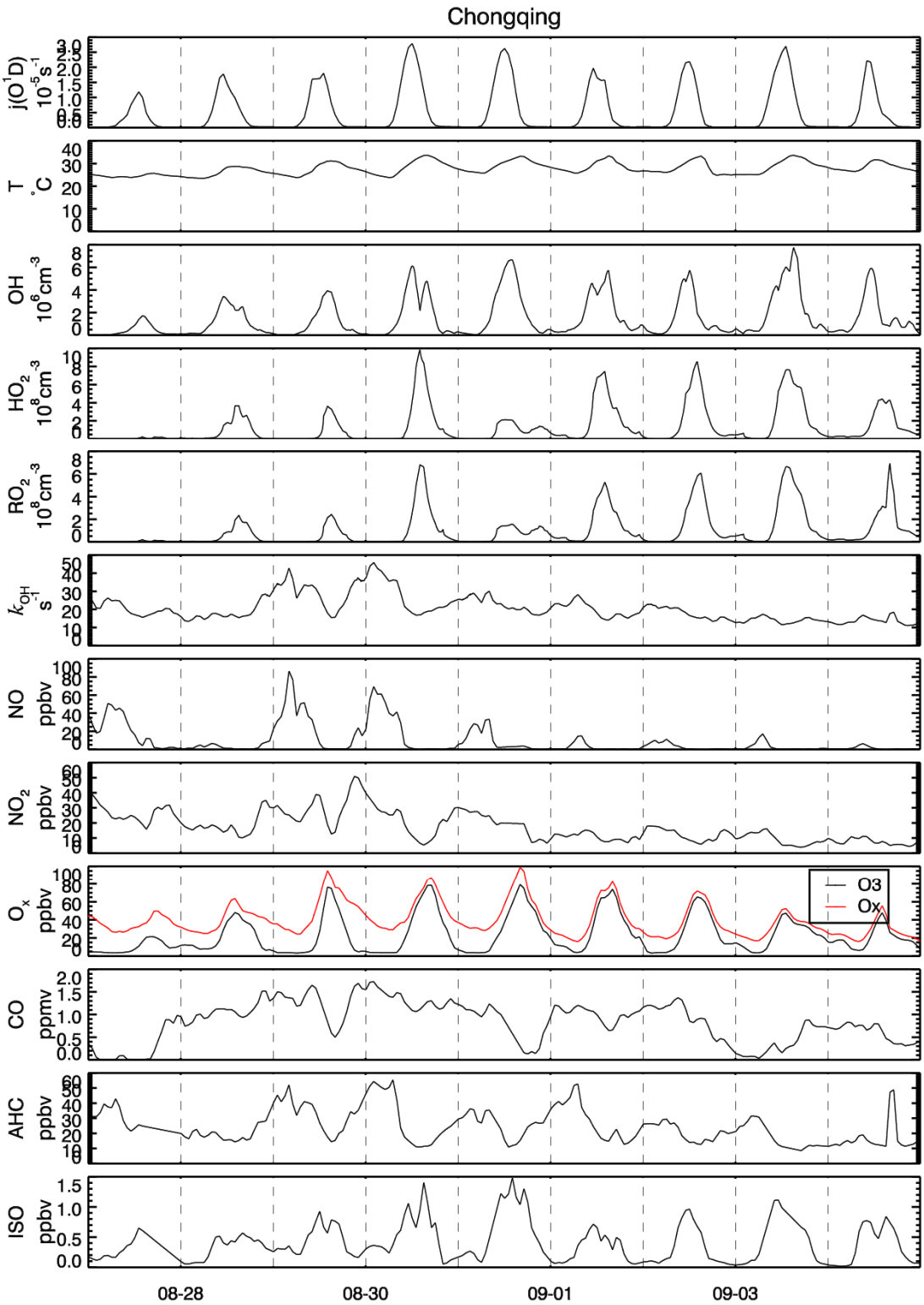

Figure S4 The time series of measured parameters (j(O^1D), Temperature, NO, NO_2, O_3, O_x, CO, AHC, isoprene) and modelled OH, HO_2, and RO_2 concentrations and OH reactivity in Chongqing.

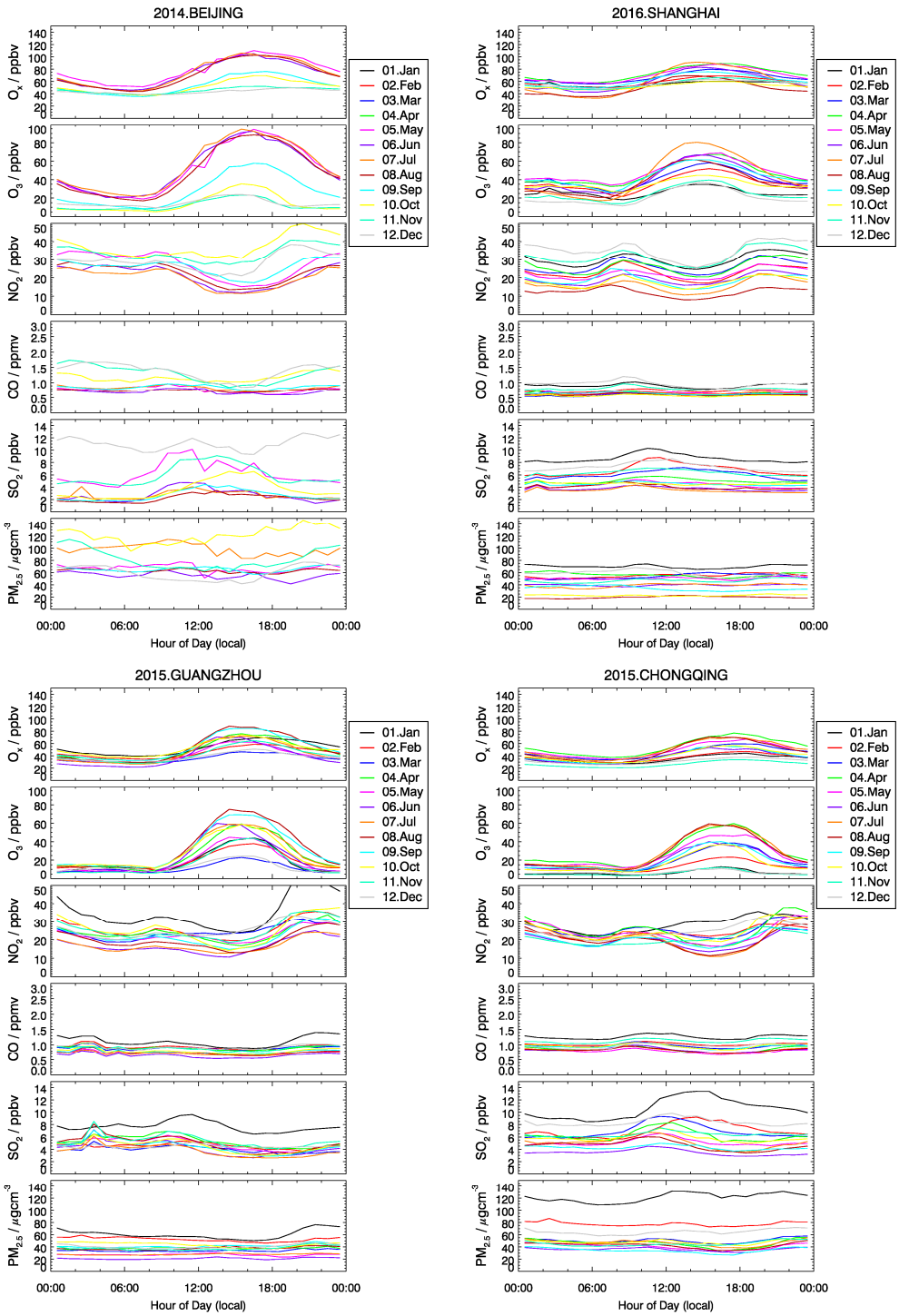

Figure S5. The monthly averaged diurnal profiles of measured O_x, O_3, NO_2, CO, PM2.5 concentrations in (a) Beijing, (b) Shanghai, (c) Guangzhou, and (d) Chongqing.

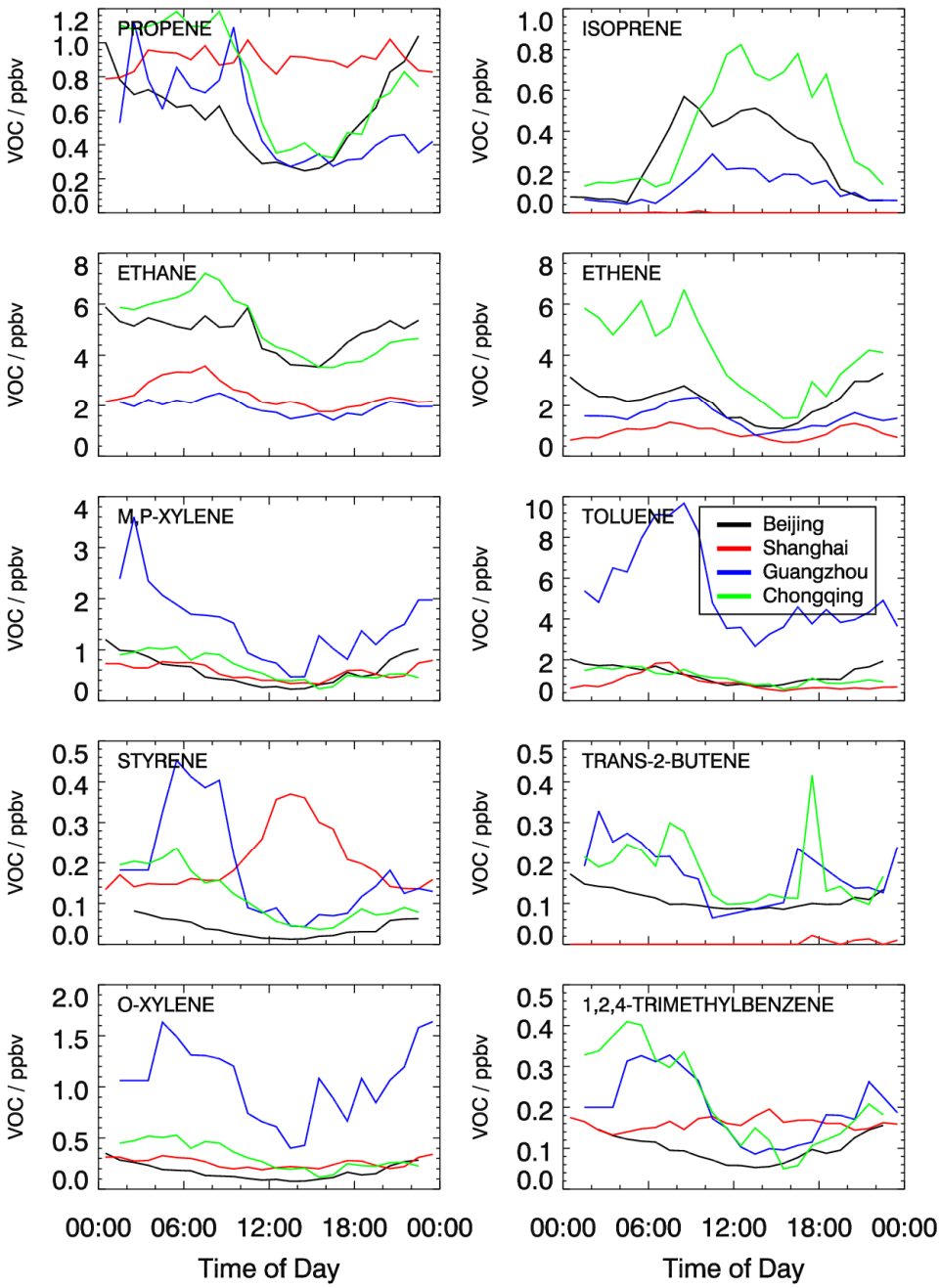

Figure S6. The mean diurnal profiles of top 10 k_{OH} contributing VOCs concentrations in Beijing, Shanghai, Guangzhou, and Chongqing.

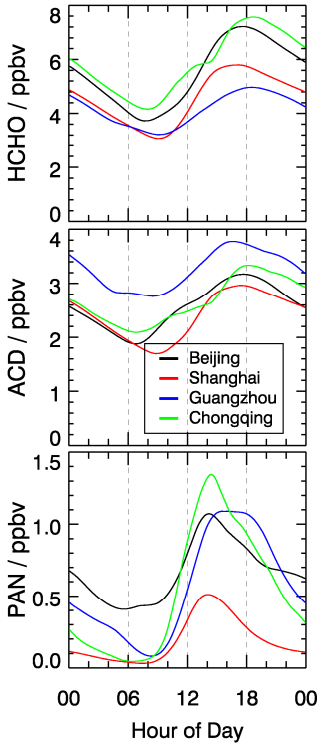

Figure S7. The mean diurnal profiles of modelled formaldehyde (HCHO), acetaldehyde (ACD) and peroxyacetyl nitrate (PAN) concentrations in four cities.

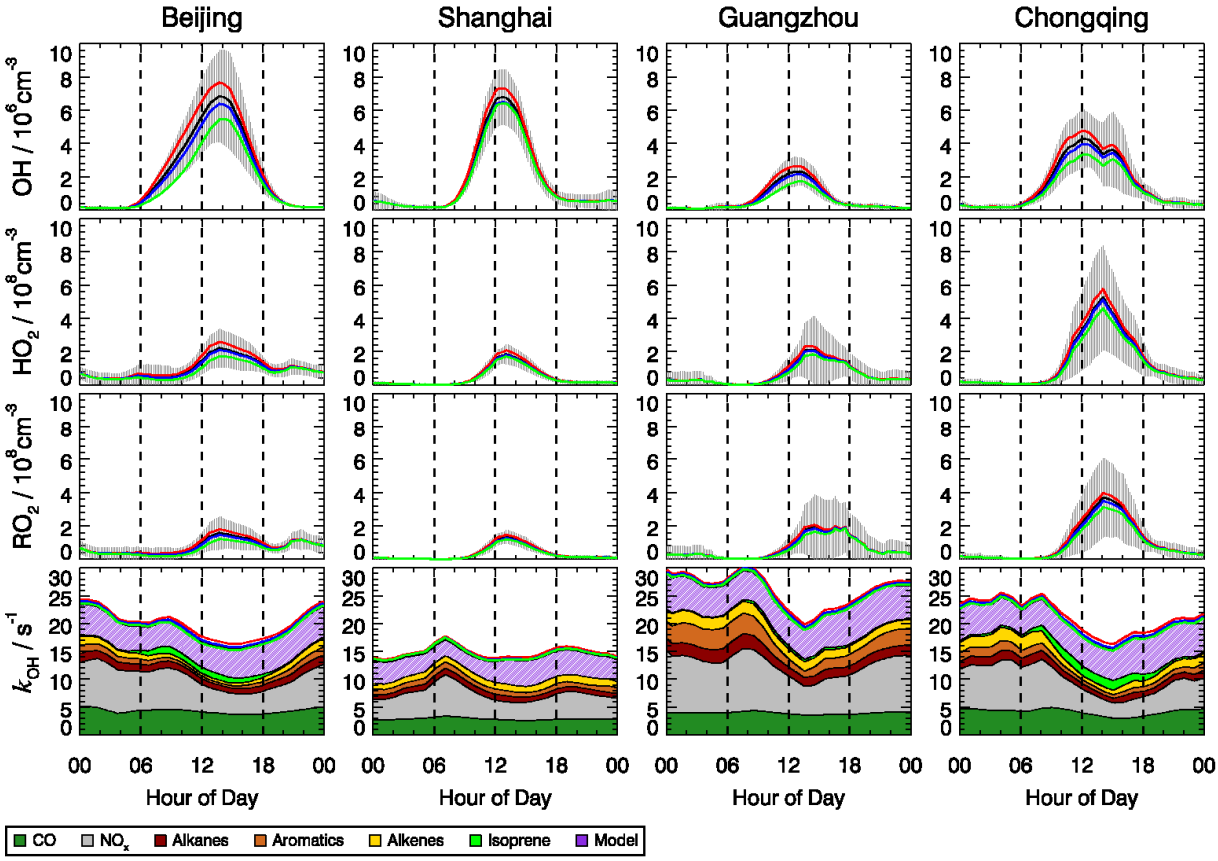

Figure S8. Mean diurnal profiles of modeled OH, HO_2, RO_2 concentrations and kOH in four measurement sites. Black: model base case (HONO=0.02*NO_2); Red: model sensitivity test M1 (HONO=0.03*NO_2); Blue: model sensitivity test M2 (HONO=0.015*NO_2); Green: model sensitivity test M3 (HONO unscaled but simulated free by the box model).

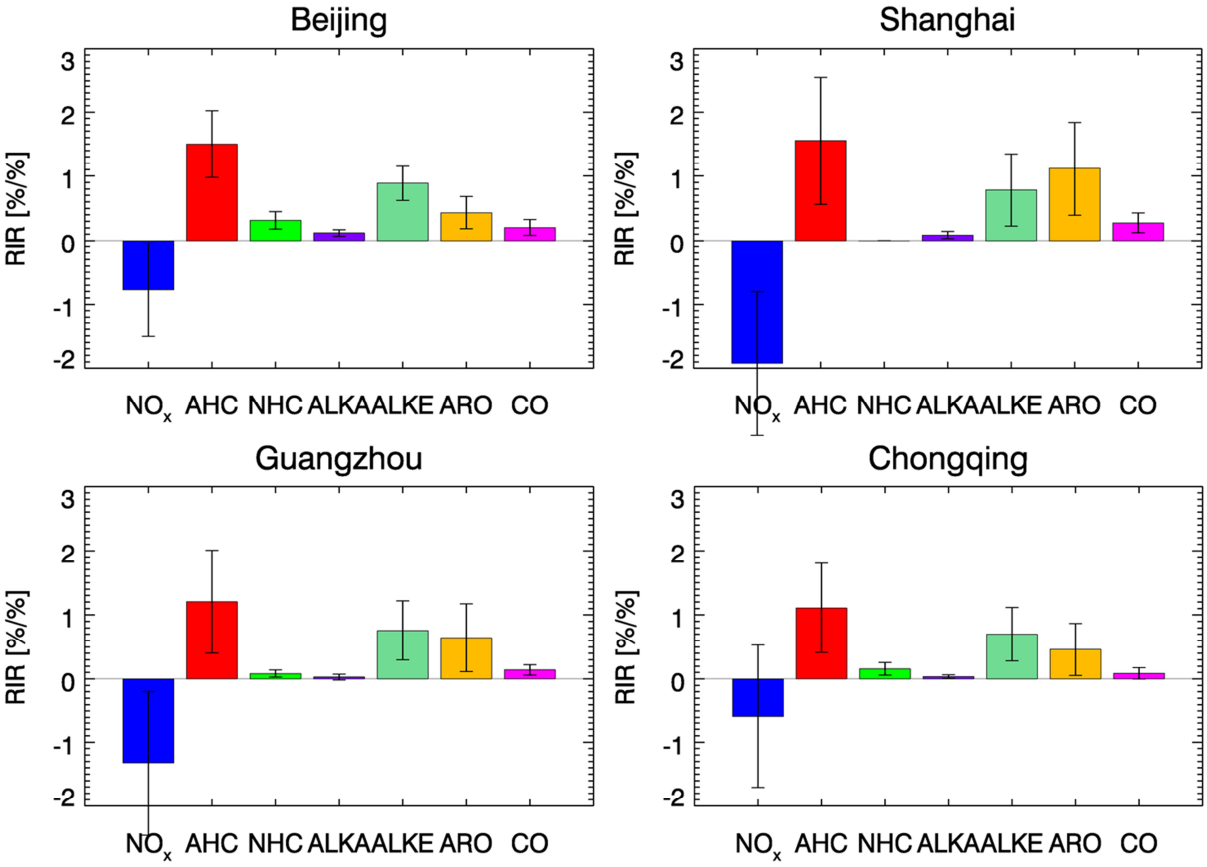

Figure S9. The RIR analysis for NO_x, AHC, CO and NHC at four sites (same as Figure 10 but HONO is free running in the model).

Reference:

Morino, Y., Kondo, Y., Takegawa, N., Miyazaki, Y., Kita, K., Komazaki, Y., Fukuda, M., Miyakawa, T., Moteki, N., and Worsnop, D.: Partitioning of HNO3 and particulate nitrate over Tokyo: Effect of vertical mixing, J. Geophys. Res., 111, D15215, https://doi.org/10.1029/2005JD006887, 2006.

Neuman, J. A., Nowak, J. B., Brock, C. A., Trainer, M., Fehsenfeld, F. C., Holloway, J. S., Hübler, G., Hudson, P. K., Murphy, D. M., Nicks, D. K., Orsini, D., Parrish, D. D., Ryerson, T. B., Sueper, D. T., Sullivan, A., and Weber, R.: Variability in ammonium nitrate formation and nitric acid depletion with altitude and location over California, J. Geophys. Res., 108, 4557, https://doi.org/doi:10.1029/2003JD003616, 2003.

Pan, Y., Tian, S., Zhao, Y., Zhang, L., Zhu, X., Gao, J., Huang, W., Zhou, Y., Song, Y., Zhang, Q., and Wang, Y.: Identifying Ammonia Hotspots in China Using a National Observation Network, Environ. Sci. Technol., 52, 3926-3934, https://doi.org/10.1021/acs.est.7b05235, 2018.

Prabhakar, G., Parworth, C. L., Zhang, X., Kim, H., Young, D. E., Beyersdorf, A. J., Ziemba, L. D., Nowak, J. B., Bertram, T. H., Faloona, I. C., Zhang, Q., and Cappa, C. D.: Observational assessment of the role of nocturnal residual-layer chemistry in determining daytime surface particulate nitrate concentrations, Atmos. Chem. Phys., 17, 14747-14770, 10.5194/acp-17-14747-2017, 2017.